Appl Nanosci (2012) 2:351–357
DOI 10.1007/s13204-012-0091-y

ORIGINAL ARTICLE

A DFT study for the structural and electronic properties of Zn_mSe_n nanoclusters

Phool Singh Yadav · Dheeraj Kumar Pandey

Received: 17 November 2011 / Accepted: 13 March 2012 / Published online: 5 April 2012

Abstract An ab initio study has been performed for the stability, structural and electronic properties of 19 small zinc selenide Zn_mSe_n ($m + n = 2$–4) nanoclusters. Out of these nanoclusters, one nanocluster is found to be unstable due to its imaginary vibrational frequency. A B3LYP-DFT/6-311G(3df) method is used in the optimization of the geometries of the nanoclusters. We have calculated the zero point energy (ZPE), which is ignored by the other workers. The binding energies (BE), HOMO–LUMO gaps and bond lengths have been obtained for all the optimized nanoclusters. For the same value of '*m*' and '*n*', we designate the most stable structure the one, which has maximum final binding energy (FBE) per atom. The adiabatic and vertical ionization potentials (IP) and electron affinities (EA), dipole moments and charge on atoms have been investigated for the most stable nanoclusters. For the same value of '*m*' and '*n*', the nanocluster containing maximum number of Se atoms is found to be most stable.

Keywords DFT study · Semiconductor · Nanoclusters · HOMO–LUMO gap

Introduction

The period for more than three decades has drawn significant attention to explore the physics and chemistry of II–VI semiconductor nanoclusters (Alivisatos 1996; Murray et al. 2000; Trindade et al. 2001; Efros and Rosen 2000; Hagfeldt and Gratzel 1995; Brus 1984). There exists a continuous transition from molecular electronic structure to that of the bulk. A nanocluster is an intermediate phase between the molecule and bulk, whose electronic and other properties may be exotic. However, two fundamental facts are attributable to the small size of these particles instead of that their physical properties are very different from those of the bulk material. The first fact is that the excitons are confined in a dimension to the order of the particle size, resulting in a compression of the bulk exciton and a corresponding blue shift in the first excited state with decreasing size (Rosetti et al. 1984). This property is known as the quantum confinement effect. According to the technological point of view, the quantum confinement effect has created a great interest due to the unique ability to tune the optical properties by changing particle size. The second important fact of these quantum-confined nanoparticles (quantum dots or QDs) is that the surface to volume ratio is much greater than that of the bulk semiconductor, and thus the nature of the surface influences more on the physical properties of these particles.

Among II–VI semiconducting materials, ZnSe is a direct band gap semiconductor with room temperature band gap energy and an emission at 2.80 eV, which suggests that ZnSe is a potentially good material for short-wavelength lasers and other photoelectronic devices. In addition, ZnSe is of special interest as it exhibits tunable-ultraviolet (UV) luminescence via quantum confinement effects. ZnSe is one of the promising materials for fabrication of light emitting devices, such as blue–green laser diodes and tunable mid-IR laser sources for remote sensing applications (Hasse et al. 1991; Jeon et al. 1991; Tawara et al. 1999; Sarigiannis et al. 2002; Rho et al. 2000; Xiang et al. 2003; Karanikolos et al. 2005; Cumberland et al. 2002).

A number of experimental (Kukreja et al. 2004; Zhu et al. 2000; Kumbhojkar et al. 1998; Reiss 2007; Nikesh

P. S. Yadav (✉) · D. K. Pandey
Department of Physics, University of Allahabad,
Allahabad 211002, India
e-mail: psycmprl@rediffmail.com

et al. 2006) and theoretical studies (Matxain et al. 2001; Deglmann et al. 2002; Goswami et al. 2006, 2007; Sanville et al. 2006) for the physical properties of both the surfaces and the bulk phases have been performed. However, a study of the small size nanoclusters of these selenides is still lacking for their better understanding in terms of the size dependence of the properties. Matxain et al. (2001) has calculated ground state geometries of small size Zn_nSe_n ($n = 1$–9) nanoclusters using B3LYP gradient-corrected density functional method. Deglmann et al. (2002) have obtained the atomic structure of Zn_nSe_n nanoclusters up to heptamers ($n = 7$). Using time-dependent (TD) density functional response theory (DFRT) within the tight-binding approach, the structural and electronic properties of unpassivated Zn_mSe_n ($m + n = 200$) clusters have been calculated by Goswami et al. (2006, 2007). Most recently, Sanville et al. (2006) produced the ZnSe nanoclusters by direct laser ablation method and analyzed in a time of flight mass spectrometer. They predicted only few physical properties like atomization energy, HOMO–LUMO gap and vertical ionization potential of small stoichiometric Zn_nSe_n ($n = 1$–16) nanocluster at B3LYP level of theory using SKBJ (d, 2df) basis set.

Earlier, we have performed an ab initio study for Ga_xN_y and Zn_xS_y nanoclusters (Yadav et al. 2007, 2010) and the study has been extended to Zn_mSe_n ($m + n = 2$–4) small nanoclusters with unequal number of n and m atoms. This study covers the other's study of Zn_mSe_n nanoclusters with equal number of n and m atoms by different method to obtain the most stable structures up to four atoms. Also, in the experimental study (Kukreja et al. 2004), most of the nanoclusters with unequal m and n atoms are found to be stable. In this paper, we report the results of a theoretical study of the structural, stabilities, HOMO–LUMO gap, adiabatic and vertical ionization potential (IP) and electron affinity (EA), charge on atoms and dipole moment of small size Zn_mSe_n ($m + n = 2$–4) nanoclusters by using the B3LYP-DFT/6-311G(3df) method. We present the method used in the investigations in second section. Third section contains the calculation and results and the last section contains the conclusions.

Methods

All the geometrical structures are fully optimized using the hybrid gradient-corrected functional (B3LYP) (Becke 1988, 1993; Lee et al. 1988) within density functional theory frame (Hohenberg and Kohn 1964; Miehlich et al. 1989) in the Gaussian-03 code (GAUSSIAN 03 et al. 2003). The harmonic vibrational frequencies of each optimized structures are determined by analytical differentiation of gradients. The polarizable triple split valance basis set, 6-311G(3df) is used as the basic basis set in this study for the most precise calculation after selecting a large number basis set for each atom. The main advantage of this split valance basis set in comparison to others is that the orbital is allowed to change its size without making any change in its shape. The three d electrons and one f electron of Zn and Se atoms are included with the valence electrons as a polarized function due to their importance for the description of the ground state of each atom in three dimensions.

Calculation and results

Stability of structures

All the possible two and three-dimensional structures have been considered for optimization to obtain a stable ground state geometry for ZnSe nanoclusters. Minimum energy for each structure is achieved by relaxing the atomic positions. In all fully optimized structures, the convergence of the system energy is obtained up to 10^{-7} meV and the forces of 10^{-3} eV/Å on each atom are achieved. We have obtained the most stable structure for each Zn_mSe_n nanocluster. The stability of nanocluster is considered on the basis of final binding energy (FBE). Quantum mechanically it is necessary to understand the zero point energy for the stability of a system. In actual calculation of binding energy of a system, it includes the zero point energy also. Therefore, a more accurate value of binding energy of a system may be obtained by subtracting the zero point energy from the calculated binding energy. Thus, for a more precise calculation, the harmonic vibrational frequencies and the corresponding zero point energy (ZPE) for all the fully optimized structures have also been calculated. The value of FBE is obtained as,

$$FBE = [(E_i - E_t)/p] - ZPE \quad (1)$$

where, E_i, E_t and p stand for the sum of the energies of all the isolated atoms present in the nanocluster, total energy of the nanocluster and the total number of atoms present in the corresponding nanocluster, respectively. All the most stable structures are presented in Fig. 1, while the symmetry, multiplicity of the ground state and the FBEs for all the optimized structures are presented in Table 1. The most stable structures have been depicted by bold letters. For the most stable structures, the calculated Se–Se, Zn–Se and Zn–Zn bond lengths are presented in Table 2. Now, we discuss each nanocluster individually as below:

ZnSe: the ground state of ZnSe nanocluster is the singlet state. The present FBE (0.52 eV) is lower than the experimental value (0.89 eV) (Weast et al. 1990). Our computed value for Zn–Se bond length of 2.22 Å is very close to the

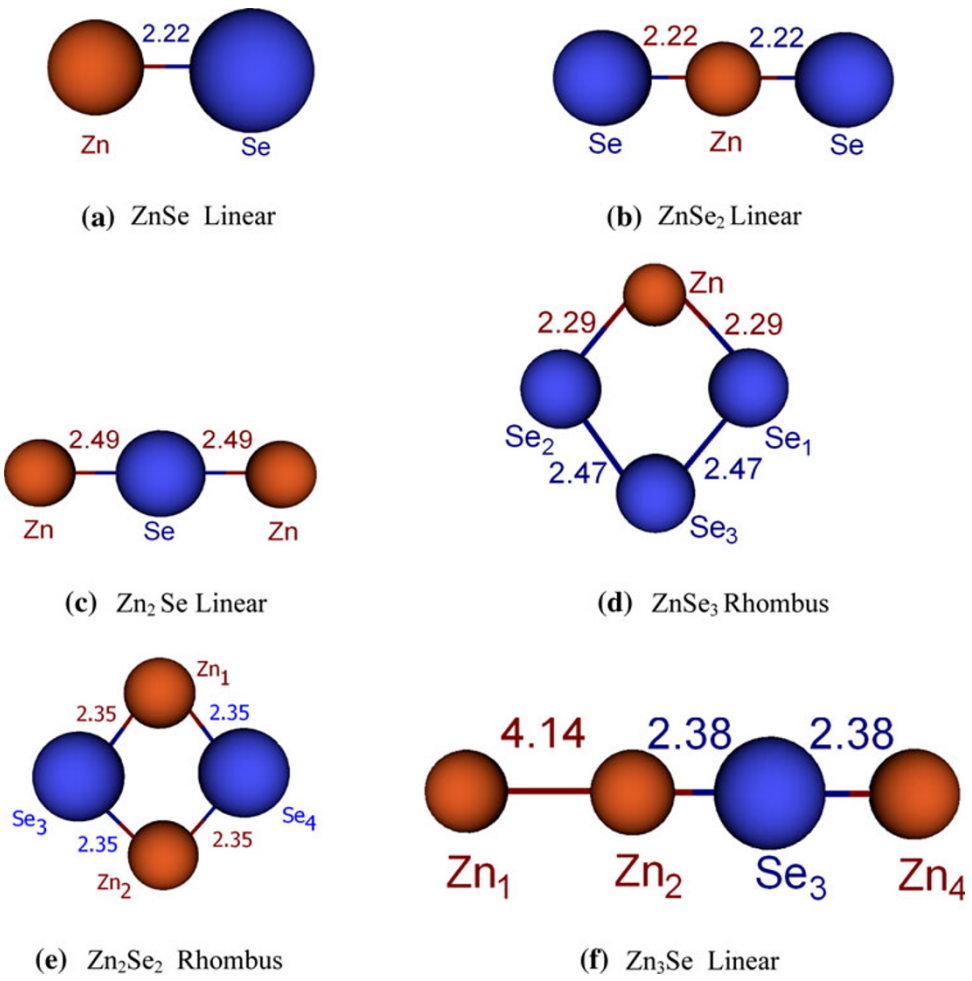

Fig. 1 Most stable structures of Zn_mSe_n $(m + n = 2–4)$ nanocluster. (All the bond lengths are in Å)

values reported by others (Matxain et al. 2001; Sanville et al. 2006) as shown in Table 2.

Zn_mSe_n $(m + n = 3)$: the ground state of three atom nanoclusters is either singlet or triplet. For $ZnSe_2$ configuration, the ground states of the linear and triangular structures are triplet and singlet, respectively, where as the reverse is true for Zn_2Se configuration.

$ZnSe_2$: we have considered the two linear structures and a triangular structure. Among them, the linear ZnSeSe has maximum FBE (1.24 eV), but it is unstable due to its imaginary frequency as shown in Table 3. The other linear SeZnSe structure having $D_{\infty h}$ symmetry has FBE of 1.22 eV and is found to be most stable. The bond length of Zn–Se of the linear SeZnSe structure is same as in linear ZnSe structure.

Zn_2Se: the investigated structures are similar to $ZnSe_2$. Among them the linear ZnSeZn structure possessing $D_{\infty h}$ symmetry has maximum FBE of 0.60 eV and is found to be most stable. For the linear ZnSeZn structure, the Zn–Se bond length is 2.49 Å as shown in Table 2. The other two structures, triangular Zn_2Se and linear ZnZnSe have lower FBEs in comparison to linear ZnSeZn structure.

Zn_mSe_n $(m + n = 4)$: all the four atom structures have the singlet and triplet ground states except the pyramidal $ZnSe_3$ structure which has pentalet ground state.

$ZnSe_3$: we have investigated five different structures like two linear chains SeZnSeSe and ZnSeSeSe, rhombus, triangular planar and pyramidal ones. The rhombus geometry having C_{2V} symmetry has maximum final binding energy of 1.72 eV and is most stable. The calculated values of Zn–Se and Se–Se bond lengths for most stable structure are 2.29 and 2.47 Å, respectively.

Zn_2Se_2: we have studied three linear chains (ZnSeZnSe, SeZnZnSe and ZnZnSeSe) and a rhombus structure. Among them, rhombus geometry having D_{2h} symmetry has maximum FBE of 1.48 eV and is found to be most stable. Sanville et al. (2006) have also reported rhombus geometry as a most stable one with binding energy of 0.68 eV. The computed Zn–Se bond length of rhombus structure is very much close to that of others (Matxain et al. 2001; Sanville et al. 2006) as shown in Table 2.

Zn_3Se: here, we have considered the three different geometries as linear chain (ZnZnSeZn), trigonal and rhombus. All the geometries have very low FBE in comparison to

Table 1 Symmetry, multiplicity of the ground state (GS), binding energy per atom (BE), zero point energy (ZPE), final binding energy (FBE) and HOMO–LUMO gap for all the configurations of Zn_mSe_n ($m + n = 2$–4) nanoclusters

Nanocluster	Configuration	Symmetry	GS Multiplicity	BE (eV)	ZPE (eV)	FBE (eV)		HOMO–LUMO Gap (eV)	
						(Present)	(Others)	(Present)	(Others)
ZnSe	**Linear ZnSe**	**$C_{\infty v}$**	**1**	**0.54**	**0.02**	**0.52**	**0.89** (Weast et al. 1990)	**1.60**	**2.58** (Weast et al. 1990), **2.41** (Luo et al. 2002), **2.69** (Luo et al. 2002)
$ZnSe_2$	Linear ZnSeSe[a]	**$C_{\infty v}$**	3	1.27	0.03	1.24		2.37	
	Linear SeZnSe	**$D_{\infty h}$**	**3**	**1.27**	**0.05**	**1.22**		**1.14**	
	Triangular SeZnSe	C_s	1	1.18	0.04	1.14		1.57	
Zn_2Se	**Linear ZnSeZn**	**$D_{\infty h}$**	**1**	**0.63**	**0.03**	**0.60**		**1.04**	
	Triangular ZnSeZn	C_{2v}	3	0.54	0.03	0.51		1.67	
	Linear ZnZnSe	**$C_{\infty v}$**	1	0.45	0.03	0.42		1.98	
$ZnSe_3$	**Rhombus**	**C_{2v}**	**1**	**1.77**	**0.05**	**1.72**		**2.37**	
	Triangular planar	C_{2v}	1	1.50	0.06	1.44		2.98	
	Linear SeZnSeSe	**$C_{\infty v}$**	3	1.36	0.06	1.30		1.00	
	Linear ZnSeSeSe	**$C_{\infty v}$**	3	1.22	0.04	1.18		1.30	
	Pyramidal	C_s	5	1.22	0.05	1.17		1.64	
Zn_2Se_2	**Rhombus**	**D_{2h}**	**1**	**1.56**	**0.08**	**1.48**	**0.68** (Sanville et al. 2006)	**2.89**	**2.69** (Sanville et al. 2006)
	Linear ZnSeZnSe	$C_{\infty v}$	3	1.09	0.05	1.04		0.00	
	Linear SeZnZnSe	$D_{\infty h}$	3	0.95	0.07	0.88		1.83	
	Linear ZnZnSeSe	$D_{\infty h}$	3	0.75	0.03	0.72		0.54	
Zn_3Se	**Linear ZnZnSeZn**	**$C_{\infty v}$**	**1**	**0.48**	**0.03**	**0.45**		**2.10**	
	Trigonal	C_{2v}	3	0.48	0.03	0.45		1.60	
	Rhombus	C_{2v}	1	0.27	0.04	0.23		1.05	

The most stable configurations are bold-faced ones. The final binding energy (FBE) = BE − zero point energy (ZPE)

[a] Unstable structure due to having at least an imaginary frequency

other structures. Among them linear ZnZnSeZn structure is most stable one with FBE of 0.45 eV and has $C_{\infty V}$ symmetry. The calculated and predicted values of Zn–Zn and Zn–Se bond lengths of linear ZnZnSeZn nanocluster are presented in Table 2.

We observe that the nanocluster containing maximum number of Se atoms for same value of '*m*' and '*n*' is most stable in comparison with others. The study also reveals that the FBE of most stable nanoclusters increases with the size of the nanocluster.

Electronic structure

The calculated energy difference between highest occupied molecular orbital and lowest unoccupied molecular orbital (HOMO–LUMO gap) for all the studied structures is presented in Table 1. The predicted HOMO–LUMO gap of ZnSe nanocluster is lower than the others (Weast et al. 1990; Luo et al. 2002) but for the rhombus Zn_2Se_2 structure, it has higher value than others (Sanville et al. 2006) as shown in Table 1. The value of HOMO–LUMO gap

increases with number of Se atoms, except for the two-atom ZnSe nanocluster.

Ionization potential and electron affinity

The ionization potential (IP) is defined as the amount of energy required to remove an electron from a nanocluster. We determine the adiabatic IP by evaluating the energy difference between the neutral and the ionized nanoclusters after finding the most stable state for the ionized nanoclusters using the optimization procedure. The electron affinity (EA) is defined as the energy released when an electron is added to a neutral nanocluster. We have determined the adiabatic EA by finding the energy difference

Table 2 Bond lengths (Å) for all the most stable configurations of Zn_mSe_n ($m + n = 2$–4) nanoclusters

Nanocluster	Configuration	Bonds	Bond length (Å)	
			(Present)	(Others)
ZnSe	Linear ZnSe (1a)	Zn–Se	2.22	2.20 (Matxain et al. 2001), 2.30 (Sanville et al. 2006)
$ZnSe_2$	Linear SeZnSe (1b)	Zn–Se	2.22	
Zn_2Se	Linear ZnSeZn (1c)	Zn–Se	2.49	
$ZnSe_3$	Rhombus (1d)	Zn–Se	2.29	
		Se–Se	2.47	
Zn_2Se_2	Rhombus (1e)	Zn–Se	2.35	2.38 (Matxain et al. 2001; Sanville et al. 2006)
Zn_3Se	Linear ZnZnSeZn (1f)	Zn–Zn	4.14	
		Zn–Se	2.38	

Table 3 The calculated vibrational frequencies (cm^{-1}), infrared intensities (IR Int. in km mol^{-1}), relative IR intensities (Rel. IR Int.) and Raman scattering activities (Raman activity in A^4/amu) of Zn_mSe_n ($m + n = 2$–4) nanoclusters

Configuration	Properties	Values
Linear ZnSe	Frequency	278
	IR Int.	0.76
	Rel. IR Int.	1.0
	Raman activity	9.27
Linear ZnSeSe	Frequencies	15i(2), 43, 372
	IR Int.	0.02, 0.10, 4.34
	Rel. IR Int.	0.00, 0.02, 1.00
	Raman activity	2.72, 13.27, 173.00
Linear SeZnSe	Frequencies	73(2), 211, 389
	IR Int.	4.31, 0.00, 14.86
	Rel. IR Int.	0.29, 0.00, 1.00
	Raman activity	0.00, 66.63, 0.00
Linear ZnSeZn	Frequencies	38(2), 161, 199
	IR Int.	11.00, 0.00, 24.72
	Rel. IR Int.	0.44, 0.00, 1.00
	Raman activity	0.00, 2.01, 0.00
Rhombus $ZnSe_3$	Frequencies	58, 62, 63, 146, 211, 347
	IR Int.	1.39, 2.75, 0.82, 0.70, 1.30, 9.79
	Rel. IR Int.	0.14, 0.28, 0.08, 0.07, 0.13, 1.00
	Raman activity	10.86, 0.03, 5.09, 15.06, 87.87, 11.39
Rhombus Zn_2Se_2	Frequencies	106, 184, 189, 224, 269, 311
	IR Int.	9.01, 21.40, 0.00, 0.00, 0.00, 29.01
	Rel. IR Int.	0.31 1.00, 0.00, 0.00, 0.00, 1.00
	Raman activity	0.00, 0.00, 3.48, 4.81, 38.55, 0.00
Linear ZnZnSeZn	Frequencies	5(2), 12, 39(2), 161, 200
	IR Int.	0.02, 0.02, 1.37, 10.74, 10.74, 1.43, 26.43
	Rel. IR Int.	0.00, 0.00, 0.05, 0.41, 0.41, 0.05
	Raman activity	16.80, 16.80, 24.32, 0.03, 0.03, 17.52, 0.41

Brackets following the frequencies contain the multiplicity of the mode

Table 4 Adiabatic and vertical ionization potential (IP) and electron affinity (EA) in eV for all the most stable configurations of Zn_mSe_n ($m + n = 2$–4) nanoclusters

The quantities given in brackets are the vertical IP and EA

Nanocluster	Configuration	IP (eV)	EA (eV)
ZnSe	Linear ZnSe (1a)	8.05 (8.09)	1.70 (1.66)
$ZnSe_2$	Linear SeZnSe (1b)	9.52 (9.63)	3.54 (3.43)
Zn_2Se	Linear ZnSeZn (1c)	7.52 (7.53)	1.40 (1.39)
$ZnSe_3$	Rhombus (1d)	7.36 (7.55)	1.75 (1.42)
Zn_2Se_2	Rhombus (1e)	7.97 (8.03)	1.58 (1.46)
Zn_3Se	Linear ZnZnSeZn (1f)	6.94 (7.42)	1.46 (1.39)

Table 5 Charge on atoms of the most stable configurations of Zn_mSe_n ($m + n = 2$–4) nanoclusters and their dipole moment (in Debye units)

The charges are distributed on the atoms in the same order of atoms as given in table

Nanocluster	Configuration	Charges on atoms				Dipole moment (Debye)
		q_1	q_2	q_3	q_4	
ZnSe	Linear ZnSe (1a)	0.789	−0.789			5.95
$ZnSe_2$	Linear SeZnSe (1b)	−0.587	1.174	−0.587		0.00
Zn_2Se	Linear ZnSeZn (1c)	0.442	−0.884	0.442		0.00
$ZnSe_3$	Rhombus ZnSeSeSe (1d)	1.146	−0.623	0.100	−0.623	3.31
Zn_2Se_2	Rhombus ZnSeSeZn (1e)	1.170	−1.170	−1.170	1.170	0.00
Zn_3Se	Linear ZnZnSeZn (1f)	0.023	0.483	−0.974	0.468	0.80

between the neutral and the anionic nanocluster. The anionic nanocluster has been relaxed to its most stable state. The adiabatic and vertical IPs and EAs for the most stable ones are included in Table 4.

The linear SeZnSe (Fig. 1b) geometry has the highest value of adiabatic IP and vertical IP as well as adiabatic and vertical EA. (Sanville et al. (2006) have reported the vertical IP for rhombus Zn_2Se_2 structure (Fig. 1e) as 8.11 eV, which is very close to our calculated value of 8.03 eV. The linear Zn_3Se configuration (Fig. 1f) has the lowest value of adiabatic and vertical IP, while linear ZnSeZn structure (Fig. 1c) has the lowest value of adiabatic EA and the lowest value of vertical EA with linear Zn_3Se (Fig. 1f) configuration. A zigzag behavior in the variation of both IP and EA with nanocluster size is observed. Neither experimental data nor earlier calculation is available for comparison of IP and EA.

Charge on atoms and dipole moment of nanoclusters

The charge on atoms of the most stable geometries of Zn_mSe_n nanoclusters and their dipole moments are depicted in Table 5. The two-atom linear ZnSe nanocluster (Fig. 1a) has highest dipole moment of 5.95 Debye due to large charge transfer between the atoms. The linear SeZnSe (Fig. 1b), linear ZnSeZn (Fig. 1c), and Zn_2Se_2 rhombus (Fig. 1e) structures have zero dipole moment due to their symmetry. The linear ZnZnSeZn (Fig. 1f) structure has quite small dipole moment. No experimental data for charge on atoms and dipole moment are available for comparison.

Conclusions

The occurrence of the most stable configurations of the various ZnSe nanoclusters has been established in the present investigations. For Zn_mSe_n nanoclusters, we have predicted the bond lengths, binding energies, HOMO–LUMO gaps, adiabatic and vertical ionization potentials and electron affinities, charge on atoms and dipole moments.

We observe that the nanocluster containing maximum number of Se atom for the same value of '*m*' and '*n*' is most stable in comparison with others. The FBEs of most stable nanoclusters also increase with the nanocluster size. The nanoclusters with high (low) FBEs have large (small) number of Se atoms. The value of HOMO–LUMO gap increases with number of Se atoms, except for the two-atom ZnSe nanocluster. We observe that the IP and EA both show zigzag behavior. The imaginary frequency causes a linear ZnSeSe structure as unstable structure, although it has the highest FBE among the $ZnSe_2$ nanoclusters. The studied most stable nanoclusters need to be grown experimentally.

Acknowledgments The authors are thankful to University Grants Commissions, New Delhi for its financial assistance.

References

Alivisatos A (1996) Perspectives on the physical chemistry of semiconductor nanocrystals. J Phys Chem 100:13226–13239

Becke AD (1988) Density-functional exchange-energy approximation with correct asymptotic behaviour. Phys Rev A 38:3098

Becke AD (1993) Density-functional thermochemistry. III. The role of exact exchange. J Chem Phys 98:5648. doi:10.1063/1.464913

Brus LE (1984) Electron–electron and electron hole interactions in small semiconductor crystallites: the size dependence of the lowest excited electronic state. J Chem Phys 80:4403

Cumberland SL, Hanif KM, Javier A, Khitrov GA, Strouse GF, Woessner SM, Yun CS (2002) Inorganic clusters as single-source precursors for preparation of CdSe, ZnSe and CdSe/ZnSe nanomaterials. Chem Mater 14:1576–1584

Deglmann P, Ahlrichs R, Tsereteli K (2002) Theoretical studies of ligand-free cadmium selenide and related semiconductor clusters. J Chem Phys 116:1585–1597

Efros AL, Rosen M (2000) The electronic structure of semiconductor nanocrystals. Annu Rev Mater Sci 30:475–521

Gaussian Inc. (2003) GAUSSIAN 03, Revision C.03 Gaussian, Pittsburgh

Goswami B, Pal S, Sarkar P, Seifert G, Springborg M (2006) Theoretical study of structural, electronic, and optical properties of Zn_mSe_n clusters. Phys Rev B 73:205312

Goswami B, Pal S, Sarkar P (2007) Theoretical studies of the effect of surface passivation on structural, electronic, and optical properties of zinc selenide clusters. Phys Rev B 76:045323

Hagfeldt A, Gratzel M (1995) Light-induced redox reactions in nanocrystalline systems. Chem Rev 95:49–68

Hasse MA, Qiu J, Depuydt JM, Cheng H (1991) Blue–green laser diodes. Appl Phys Lett 59:1272–1574

Hohenberg P, Kohn W (1964) Inhomogeneous electron gas. Phys Rev B 136:B864–B871

Jeon H, Ding J, Patterson W, Nurmikko AV, Xie W, Grillo DC, Kobayashi M, Gunshor RL (1991) Blue–green injection laser diodes in (Zn, Cd)Se/ZnSe quantum wells. Appl Phys Lett 59:3619–3621

Karanikolos GN, Alexandridis P, Mallory R, Petrou A, Mountziaris TJ (2005) Synthesis of ZnSe nanostructures using lytropic liquid crystals. Nanotechnology 16:2372

Kukreja LM, Rohlfing A, Misra P, Hillenkamp F, Dreisewerd K (2004) Cluster formation in UV laser ablation plumes of ZnSe and ZnO studied by time-of-flight mass spectrometry. Appl Phys A Mater Sci Process 78:641–644

Kumbhojkar N, Mahamumi S, Leppert V, Risbud SH (1998) Quantum confinement effects in chemically grown, stable ZnSe nanoclusters. Nanostruct Mater 10(2):117–129

Lee C, Yang W, Parr RG (1988) Development of the Colle-Salvetti correlation-energy formula into a functional of the electron density. Phys Rev B 371:785

Luo W, Ismail-Beigi S, Cohen ML, Louie SG (2002) Quasiparticle band structure of ZnS and ZnSe. Phys Rev B 66:195215

Matxain JM, Mercero JM, Fowler JE, Ugalde M (2001) Small clusters of group-II–VI materials: Zn_iX_i, X = Se, Te, i = 1–9. Phys Rev A 64:053201

Miehlich B, Savin A, Stoll H, Preuss H (1989) Results obtained with the correlation energy density functionals of Becke and Lee, Yang and Parr. Chem Phys Lett 157:200

Murray CB, Kagan CR, Bawendi MG (2000) Synthesis and characterization of monodisperse nanocrystals and close-packed nanocrystal assemblies. Annu Rev Mater Sci 30:545–610

Nikesh VV, Lad AD, Kimura S, Nozaki S, Mahamuni S (2006) Electron energy levels in ZnSe quantum dots. J Appl Phys 100:113520

Reiss P (2007) ZnSe based colloidal nanocrystals: synthesis, shape control, core/shell, alloy and doped systems. New J Chem 31:1843–1852. doi:10.1039/b712086a

Rho H, Jackson HE, Lee S, Dobrowolska M, Furdyna JK (2000) Raman scattering from CdSe/ZnSe self-assembled quantum dot structures. Phys Rev B 61:15641

Rosetti R, Ellison JL, Gibson JM, Brus LE (1984) Size effects in the excited electronic states of small colloidal CdS crystallites. J Chem Phys 80:4464

Sanville E, Burnin A, Belbruno J (2006) Experimental and computational study of small (n = 1–16) stoichiometric Zinc and Cadmium chalcogenide clusters. J Phys Chem A 110(7):2378–2386. doi:10.1021/jp056218v

Sarigiannis D, Peck JD, Kioseoglou G, Petrou A, Mountziaris TJ (2002) Characterization of vapour-phase-grown ZnSe nanoparticles. Appl Phys Lett 80:4024–4026

Tawara T, Tanaka S, Kumano H, Suemune I (1999) Growth and luminescence properties of self-organized ZnSe quantum dots. Appl Phys Lett 75:235

Trindade T, O'Brien P, Pickett NL (2001) Nanocystalline semiconductor: synthesis, properties and perspectives. Chem Mater 13:3843–3858

Weast RC, Lide DR, Astle MJ, Beyer WH (1990) CRC handbook of chemistry and physics, 70th edn. Chemical Rubber, Boca Raton

Xiang B, Zhang HZ, Li GH, Yang FH, Su FH, Wang RM, Xu J, Lu GW, Sun XC, Zho Q, Yu DP (2003) Green-light- emitting ZnSe nanowires fabricated via vapour phase growth. Appl Phys Lett 82:3330

Yadav PS, Yadav RK, Agrawal BK (2007) Structural, electronic and vibrational properties of small GaxNy (x + y = 2–5) nanoclusters: a B3LYP-DFT study. J Phys Condens Mater 19:076209

Yadav PS, Pandey DK, Agrawal S, Agrawal BK (2010) Ab initio study of structural, electronic, optical and vibrational properties of Zn_xS_y (x + y = 2 to 5) nanoclusters. J Nanopart Res 12:737–757

Zhu J, Koltypin Y, Agrawal S, Gedanken A (2000) General sonochemical method for the preparation of nanophasic selenides: synthesis of ZnSe nanoparticles. A Chem Mater 12:73